RESEARCH PAPER

Level set based robust shape and topology optimization under random field uncertainties

Shikui Chen · Wei Chen · Sanghoon Lee

Abstract A robust shape and topology optimization (RSTO) approach with consideration of random field uncertainty in loading and material properties is developed in this work. The proposed approach integrates the state-of-the-art level set methods for shape and topology optimization and the latest research development in design under uncertainty. To characterize the high-dimensional random-field uncertainty with a reduced set of random variables, the Karhunen–Loeve expansion is employed. The univariate dimension-reduction (UDR) method combined with Gauss-type quadrature sampling is then employed for calculating statistical moments of the design response. The combination of the above techniques greatly reduces the computational cost in evaluating the statistical moments and enables a semi-analytical approach that evaluates the shape sensitivity of the statistical moments using shape sensitivity at each quadrature node. The applications of our approach to structure and compliant mechanism designs show that the proposed RSTO method can lead to designs with completely different topologies and superior robustness.

Keywords Robust design · Topology optimization · Shape optimization · Level set methods · Uncertainty · Random field · Dimension reduction

Nomenclature

$C(x_1, x_2)$	spatial covariance function
$\mathbf{D}$	spatial domain
E_{ijkl}	elastic tensor
$a(x, \omega)$	random field
$\bar{a}(x)$	mean function of $a(x, \omega)$
$a_i(x)$ or $\mathbf{a_i}$	ith eigenfunction of random field
$g(\mathbf{z})$	function of $\mathbf{z}$
J	objective functional
$p(z)$	joint probability density function
u	state variable
$\mathbf{V}(x)$	design velocity field
w_i	weight of the ith quadrature point
ϕ	level set function
λ	Lagrange multiplier
λ_i	ith eigenvalue of random field
$\xi_i(\omega)$	orthogonal random variables with zero mean and unit variance
μ	mean performance
σ^2	performance variance
$\mathbf{z}$	vector of random variables
z_i	the i-th random variable of $\mathbf{z}$
z_{ij}	the j-th quadrature node of z_i
Θ	sample space
ω	an element of sample space Θ
Ω	geometric shape of design
$\partial\Omega$	boundary of Ω

S. Chen · W. Chen (✉)
Department of Mechanical Engineering, Northwestern University,
2145 Sheridan Road, Evanston, IL, USA
e-mail: weichen@northwestern.edu

S. Lee
Korea Atomic Energy Research Institute, 1045 Daedeok-Daero,
Yuseong-gu, Daejeon, Republic of Korea

1 Introduction

Since the seminal work of Bendsøe and Kikuchi (1988), structural topology optimization has undergone considerable developments during the past two decades, which

provides an efficient way to obtain effective design candidates and greatly accelerates the engineering design innovation process. The state-of-the-art topology optimization approaches include the ground structure method (Bendsøe et al. 1994), the homogenization based method (Bendsøe and Kikuchi 1988), simple isotropic material with penalization (SIMP) (Rozvany et al. 1992; Sigmund 2001), and the level set methods (Wang et al. 2003; Allaire et al. 2004). Although topology optimization is becoming a matured field, most of the current work is focused on deterministic optimization where the design is determined without consideration of various sources of uncertainties, such as the variation in the loading, material properties, or geometric variations due to the imprecise manufacturing process. To obtain robust and reliable designs, the uncertainties existing in the structure and its operating environment need to be considered and their impact on design performance should be assessed quantitatively during a design process. Topology optimization under uncertainties is still an open research area which requires further investigations. The difficulties are largely attributed to the infinite-dimensional property of topology optimization, which poses great challenges in uncertainty representation, propagation, and design sensitivity analysis.

Recent years have seen growing interests in taking uncertainty into account to obtain robust and reliable topological designs. Due to its simplicity, frame structures were first studied for robust and reliability-based topology optimization under uncertainty (Christiansen et al. 2001; Mogami et al. 2006; Seepersad et al. 2006; Jung and Cho 2004). Olhoff et al. first integrated reliability analysis into the element-based topology optimization method and introduced a new strategy called reliability-based topology optimization (RBTO) (Kharmanda and Olhoff 2002), where a probabilistic constraint is introduced and the objective is treated as deterministic. Reliability-based topology optimization was further developed in recent years by different research groups (Jung and Cho 2004; Maute and Frangopol 2003; Kharmanda et al. 2004; Allen and Maute 2005). A comprehensive review of RBTO can be found in Mozumder et al. (2006). On the other hand, not many works, except Seepersad et al. (2006), Kogiso et al. (2008), Conti et al. (2008), exist on robust topology optimization (RTO), although it is a topic of great significance both in academic and industrial applications.

Robust optimization problems have been addressed in different scientific disciplines (Beyer and Sendhoff 2007). The first approach is the method of stochastic programming (Birge and Louveaux 1997) with its root in operations research; the second method is robust design (Chen et al. 1996) that originated in engineering design. Among the existing RTO works, Seepersad et al. employed the frame

structure method and the robust design approach to implement robust topology optimization of cell structures considering uncertain boundary conditions (Seepersad et al. 2006). The limitation in the frame-structure based RTO method lies in the fact that the configuration of the optimal design is determined to a large extent by the number and locations of the nodes of the frame structure. If the number of nodes is limited, the solution may not be sufficient to represent the optimal topology. Using the homogenization based method, Kogiso et al. (2008) proposed a sensitivity-based RTO method for designing compliant mechanisms, where the effect of the variations in the direction of the input force on the output displacement is considered based on the first-order derivative. Conti's work (2008) is the first to combine level set methods with stochastic programming techniques for structural optimization, however, the work is limited to considering only the loading uncertainty in a random variable form.

In this work, we propose a methodology for robust shape and topology optimization (RSTO) problems by integrating the level set methods with the robust design formulation considering not only the random variable uncertainty, but also random field uncertainties in loading and material properties. Conventional robust design optimization is usually set as a continuous optimization problem in finite dimensions. To combine robust design with shape and topology optimization, which is an infinite-dimensional optimization problem, we define the statistical moments of the response as functionals of geometric shapes and a set of random variables reduced from random field. A fundamental challenge to be addressed in RSTO is how to characterize uncertainties and propagate them to the design responses in an efficient manner. In this paper, the spectral method (Ghanem and Spanos 1991), in particular the Karhunen–Loeve expansion, is employed to reduce the dimensionality in uncertainty representation. In addition, the statistical moments of design responses are evaluated using the generalized Gauss-type quadrature, which transforms the RTO problem into a weighted summation of a series of deterministic topology optimization sub problems at the quadrature nodes. The design (shape) sensitivity is derived at each quadrature node using the adjoint variable method. The shape derivative is further combined with a steepest descent method to form a design velocity filed for the level set equation to update the design solution in optimization iterations. The level set methods offer a precise boundary description for implementing both the robust shape optimization and topology optimization in a unified mathematical framework, which is another advantage of the proposed method.

This paper is organized as follows: A brief review of robust optimization and fundamentals about level set methods for RSTO are presented in Section 2. After that,

uncertainty characterization and propagation using the spectral method and the Gauss-type quadrature are introduced in Section 3. In Section 4, the shape derivatives of the statistical moments are evaluated using the adjoint variable method. The numerical algorithm for RSTO together with four demonstration examples is provided in Section 5. Conclusions and future works are discussed in the last section.

2 Level-set based RSTO

2.1 Robust design models

Conventional robust design, pioneered by Taguchi (1993), refers to a class of methods for improving quality and reliability by designing a product or process so that it is robust (insensitive) against variations in uncontrollable noise variables (Phadke 1989; Wu and Hamada 2000). The robust design problem typically involves a nonlinear programming formulation (Chen et al. 1996; Parkinson et al. 1993) in which the objective is to make suitable tradeoff between 'optimizing' the mean performance μ and minimizing the performance variance σ^2 (or the standard deviation σ), as shown in Fig. 1.

The common robust design objective function balances between the mean and standard deviation of the objective response through the choice of the constant k (Kalsi et al. 2001; Jin et al. 2003). Functions of the form $\mu + k\sigma$ also play a role when we have constraint responses that must satisfy certain conditions with specified probabilities. When the constraints relate to the failure of a product, the constraint evaluation is often referred to as reliability assessment (Melchers 1999; Du and Chen 2000, 2001). A complete review of robust design optimization can be found in literatures (Beyer and Sendhoff 2007; Chen et al. 1996).
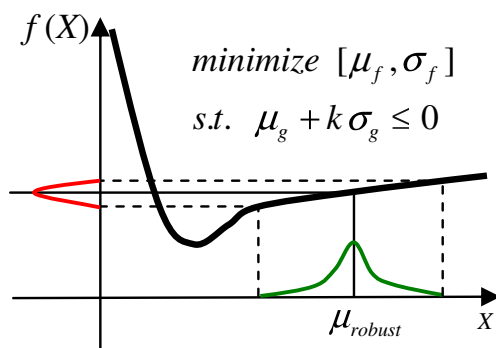

$$minimize \ [\mu_f, \sigma_f]$$
$$s.t. \ \ \mu_g + k\sigma_g \leq 0$$

Fig. 1 Robust design model (Chen et al. 1996)

2.2 Level set methods for shape and topology optimization

Level set methods were originally introduced by Osher and Sethian (1988) as a numerical scheme for tracking fronts propagating with curvature-dependent speed. In the past two decades, level set methods have thrived to be powerful tools with many applications in different fields (Sethian 1999; Osher and Fedkiw 2003). Their advantage lies in their capability of precisely describing closed boundaries with dynamic variations, which enables easy 'capture' of the boundary on a fixed Eulerian grid (a structured rectangular grid) by solving a Hamilton–Jacobi partial differential equation (Wang et al. 2003). Sethian and Wiengmann (2000) first combined level set methods with the immersed interface methods for structural boundary design, where the former was used to represent the geometric boundary of the design and the latter was used for elastic analysis. Osher and Santosa (2001) introduced the shape gradient of the objective functional into the level set model and established a link between the shape gradient and the velocity field. This work was further completed by Allaire et al. (2002, 2004), who derived the shape sensitivity of compliance and geometric advantage by employing the adjoint variable method. Starting from the material time derivative method (Wang et al. 2003; Wang and Wang 2004b), Wang et al. (2003) identified a meaningful link between the velocity field in the level set method and the general structural sensitivity analysis. The 'color level set' model, which was also proposed by Wang (2004b), made possible the topology optimization of multi-material structures and compliant mechanisms in the level set framework (Wang and Wang 2004a; Wang et al. 2005; Chen and Wang 2007; Chen et al. 2008; Wang and Chen 2009). To avoid being lost in technical details, in this section, we only focus on the key issues involved in RSTO. A complete introduction to level set methods can be found in Sethian (1999), Osher and Fedkiw (2003).

As its name implies, level set method implicitly represents the boundary as the zero level set of a one-higher dimensional surface $\phi(x)$, which is called the level set function. In the level set model, the domain is defined as three parts according to the value of the level set function:

$$\begin{cases} \phi(x(t)) > 0 & : & x(t) \in D \backslash \Omega \\ \phi(x(t)) = 0 & : & x(t) \in \partial\Omega \\ \phi(x(t)) < 0 & : & x(t) \in \Omega \backslash \partial\Omega \end{cases}, \qquad (1)$$

where D denotes the design domain; and $t \in R^+$ is time. The domain and a sketch of level set representation are shown in Fig. 2. The greatest advantage of implicit representation lies in its ability of dealing with topological changes,

(a) 3D level set function

(b) corresponding 2D geometry
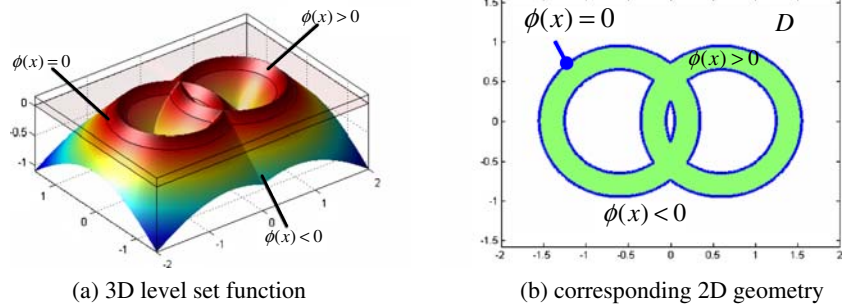
such as splitting and merging of the boundary, in a natural manner.

By calculating the material time derivative (Reddy 1986) of the equation $\phi(x) = 0$, we get the following equation:

$$\frac{\partial \phi}{\partial t} + \nabla \phi \cdot \mathbf{V}(x) = 0, \tag{2}$$

where $\mathbf{V}(x) = \frac{dx}{dt}$ is the velocity vector field. Considering $\mathbf{n} = \frac{\nabla \varphi}{|\nabla \varphi|}$ and $\mathbf{V} \cdot \nabla \varphi = (\mathbf{V} \cdot \mathbf{n}) |\nabla \varphi|$, we can write (2) as

$$\frac{\partial \phi}{\partial t} + V_n(x) |\nabla \phi| = 0. \tag{3}$$

These two Hamilton–Jacobi type partial differential equations (PDEs) are the well-known level set equations (Osher and Sethian 1988; Sethian 1999; Osher and Fedkiw 2003). Based on the level set theory, the topology optimization problem is transformed into a problem of finding the steady-state solution of the Hamilton–Jacobi equation. To get a feasible steady-state solution of (2) and (3), an important issue is to identify a rational velocity field. More details on calculating the shape derivative and identifying the velocity field in the RSTO problem will be provided in Section 4.

2.3 Setting an RSTO problem

In probabilistic RSTO, uncertainty is introduced as a new dimension in addition to space and time (Zabaras 2007), while the solution is sought in this extended space. Let's use $\mathbf{z}$ to denote the random variables in the system, and assume $\mathbf{z}$ is independent of the design variable, shape Ω. The design response (performance) under uncertainties can be correspondingly expressed as a functional $J(\Omega, \mathbf{u}, \mathbf{z})$ of the random quantities $\mathbf{z}$ in addition to the geometric shape Ω and state variable $\mathbf{u}$, that is

$$J(\Omega, \mathbf{u}, \mathbf{z}) = \int_\Omega f(\mathbf{u}(\Omega, \mathbf{z})) d\Omega, \tag{4}$$

where the performance function $J(\Omega, \mathbf{u}, \mathbf{z})$ is the total strain energy, or the mean compliance of the structure in structural optimization; in complaint mechanism optimization, $J(\Omega, \mathbf{u}, \mathbf{z})$ is the geometric advantage or work efficiency. The random quantities involved in the system can have spatial variability to form a random field or random process but it can always be discretized into a finite number of random variables, which will be further explained in Section 3.1. Thus (4) is general enough to cover random field or random process.

The mean $\mu(J(\Omega, \mathbf{u}, \mathbf{z}))$ and standard derivation $\sigma(J(\Omega, \mathbf{u},\mathbf{z}))$ of the response $J(\Omega, \mathbf{u}, \mathbf{z})$ in (4) can be further expressed as follows:

$$\mu(J(\Omega, \mathbf{u}, \mathbf{z})) = \iint_\Omega p(\mathbf{z}) f(\mathbf{u}(\Omega, \mathbf{z})) d\Omega d\mathbf{z}$$
$$= \int p(\mathbf{z}) J(\Omega, \mathbf{u}, \mathbf{z}) d\mathbf{z},$$
$$\sigma^2(J(\Omega, \mathbf{u}, \mathbf{z})) = \int p(\mathbf{z}) \left[\int_\Omega p(\mathbf{z}) f(\mathbf{u}(\Omega, \mathbf{z})) d\Omega \right.$$
$$\left. - \iint_\Omega p(\mathbf{z}) f(\mathbf{u}(\Omega, \mathbf{z})) d\Omega d\mathbf{z} \right]^2 d\mathbf{z}$$
$$= \int p(\mathbf{z}) \left[J(\Omega, \mathbf{u}, \mathbf{z}) - \mu(J(\Omega, \mathbf{u}, \mathbf{z})) \right]^2 d\mathbf{z}, \tag{5}$$

where $p(\mathbf{z})$ is the joint probability density function (p.d.f.) of the random variables. In this way, an RSTO problem is set as follows:

Minimize
$$J^*(\Omega, \mathbf{u}, \mathbf{z}) = \mu(J(\Omega, \mathbf{u}, \mathbf{z})) + k\sigma(J(\Omega, \mathbf{u}, \mathbf{z}))$$
Subject to :
$$Volume\ constraint\ |\Omega| = |\Omega|_{obj},$$
$$Perimeter\ constraint\ on\ |\partial \Omega|, \tag{6}$$

together with the partial differential equations (PDEs) governing the physical system.

3 Uncertainty quantification and propagation in RSTO

3.1 Random variable and random field

Uncertainties in structural optimization can be modeled either by *random variables* or *random fields* (Ying et al. 2009). The former can be considered as the constituting element of the latter, as shown in Fig. 3. Random variables and random fields can be used to model different physical quantities. For example, when considering a concentrated random load, we can model its magnitude and direction as two random variables (Chen et al. 2009), either correlated or independent. But for physical quantities varying across the spatial domain, e.g., material property or a distributed random load, they should be more realistically modeled as random fields (Ying et al. 2009). A random variable often can be conveniently characterized by the mean and standard deviation of its distribution. To characterize a random field, a third factor needs to be taken into account, that is, the correlations (dependency) among the random variables in this random field. When there is no correlation or the correlation is very weak, the random field is more like the 'white noise' in signal analysis and Monte Carlo method can be used to model such a random field. When the correlation is strong, spectral methods (Ghanem and Spanos 1991) need to be employed to quantify the uncertainty. In this work, we use a Gaussian random field with a relatively strong correlation to describe the uncertain material field. To characterize the random-field material uncertainty with a reduced set of random variables, the Karhunen–Loeve (K–L) expansion approach is employed. To efficiently propagate uncertainty in a RSTO process, we propose to use the univariate dimension reduction (UDR) method which is applicable to arbitrary probability distributions. The uncertainty modeled by a random field needs to be discretized into a finite number of random variables for practical manipulations. In this section, we first discuss the discretization of random fields using the K–L spectral representation and the propagation of uncertainty based on the UDR method combined with quadrature formula for sampling. These methods are further incorporated into the framework of the level-set based RSTO.

3.2 Reduced order Karhunen–Loeve expansion of random field

The Karhunen–Loeve expansion (Ghanem and Spanos 1991) is a spectral approach to represent a random field using eigenfunctions of the random field's covariance function as expansion bases. Let $a(x, \omega) : \mathbf{D} \times \Theta \rightarrow \mathbb{R}$ be a random field defined over a spatial domain $\mathbf{D}$, which is a function of spatial coordinate x. Here $\omega \in \Theta$ denotes an element of the sample space and is used to indicate that the involved quantity is random. The random field $a(x, \omega)$ can be represented by the K–L expansion as follows:

$$a(x, \omega) = \bar{a}(x) + \sum_{i=1}^{\infty} \sqrt{\lambda_i} a_i(x) \xi_i(\omega), \tag{7}$$

where $\bar{a}(x)$ is the mean function. λ_i and $a_i(x)$ are the ith eigenvalue and eigenfunction obtained from the following integral equation:

$$\int_{\mathbf{D}} C(x_1, x_2) a_i(x_1) \, dx_1 = \lambda_i a_i(x_2), \tag{8}$$

where $C(x_1, x_2)$ is the spatial covariance function of the random field $a(x, \omega)$. The random field variables, $\xi_i(\omega)$ in (7)
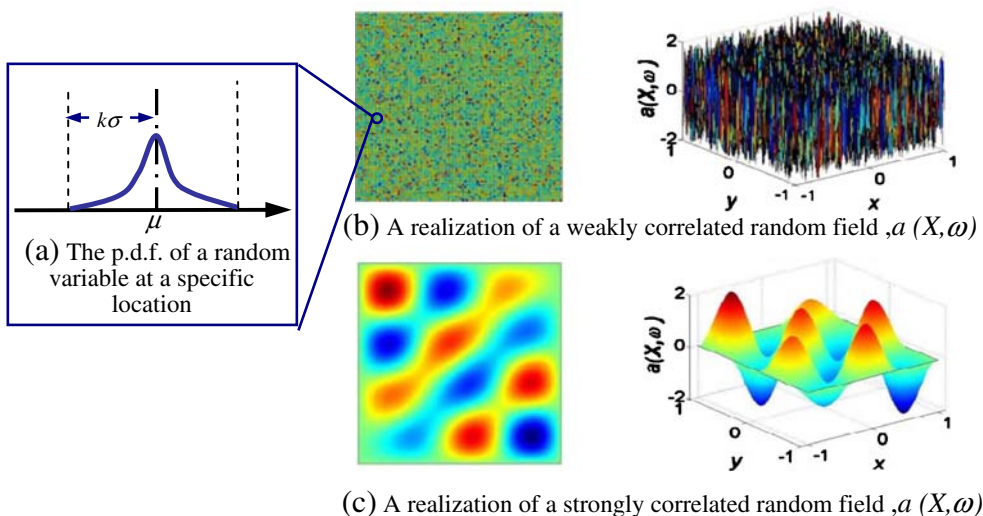

(a) The p.d.f. of a random variable at a specific location

(b) A realization of a weakly correlated random field ,$a(X, \omega)$

(c) A realization of a strongly correlated random field ,$a(X, \omega)$

Fig. 3 **a–c** Concept of random variable and random field

are orthogonal random variables with zero mean and unit variance. That is,

$$E\left(\xi_i\left(\omega\right)\right) = 0 \quad \text{and} \quad E\left(\xi_i\left(\omega\right)\xi_j\left(\omega\right)\right) = \delta_{ij}. \tag{9}$$

The orthogonality of $\xi_i(\omega)$ is a unique feature of the K–L expansion. $\xi_i(\omega)$ can be calculated as:

$$\xi_i\left(\omega\right) = \frac{1}{\sqrt{\lambda_i}} \int_D \left(a\left(x, \omega\right) - \bar{a}\left(x\right)\right) a_i\left(x\right) dx. \tag{10}$$

The second order statistics of $\xi_i(\omega)$ in (9) can be derived from (10) Based on sampling and spatial integration at the right side of (10), samples of $\xi_i(\omega)$ can be generated to infer the distribution of the random field variable, $\xi_i(\omega)$. The K–L expansion is the optimal among finite representations using orthogonormal bases in the sense that the mean square error caused by a truncation of the expansion is minimized (Ghanem and Spanos 1991).

When applying the K–L expansion to a discretized random field, operations on functions are transformed into operations on matrices (Ghanem and Doostan 2006). A random field can be spatially discretized by the spatial averaging method or the collocation method (Haldar and Mahadevan 2000). Let $\mathbf{a}(\omega)$ denote an N dimensional random vector whose elements are random variables obtained by discretizing a random field $a(x, \omega)$ at N observation points in the domain **D**. The K–L expansion of $\mathbf{a}(\omega)$ can be expressed as:

$$\mathbf{a}\left(\omega\right) = \bar{\mathbf{a}} + \sum_{i=1}^{N} \sqrt{\lambda_i} \mathbf{a}_i \xi_i\left(\omega\right), \tag{11}$$

where $\bar{\mathbf{a}}$ denotes a vector containing the mean values of the random field at the N observation points; λ_i and $\mathbf{a}_i$ are the eigenvalues and eigenvectors of the covariance matrix C; $\xi_i(\omega)$ are orthogonal random field variables with zero mean and unit variance. By truncating (11) at some $M \ll N$, a reduced order K–L representation of random field can be obtained with its significance of representing the random field measured as:

$$s = \sum_{i=1}^{M} \lambda_i \bigg/ \sum_{i=1}^{N} \lambda_i. \tag{12}$$

When s is sufficiently close to one, a reduced order representation ((11) with $N = M$) can be used to represent the random field with a much smaller dimensionality (M) without sacrificing too much accuracy. The random field variables $\xi_i(\omega)$ thus identified with reduced dimensionality together with other random quantities in the system,

comprise the vector of random variables, denoted as z in the optimization formulation (4). The benefits of such reduction will be further demonstrated in our example problems. The procedure illustrated above can also be used to characterize a random field from data obtained at a finite number of observation points in a spatial domain (Ghanem and Doostan 2006).

3.3 Multivariate gauss-type quadrature for statistical moments calculation

Multivariate quadrature formulas for multiple random variables can be built from one dimensional quadrature formulas. There are many ways of doing this (Engels 1980) and in this paper, we focus our examination on two methods, the tensor product quadrature (TPQ) formula and the univariate dimension reduction (UDR) method.

With the TPQ formula, the k-th statistical moments of $g(\mathbf{z})$ can be calculated as:

$$E[g^k] = \int_{\Omega_1} \cdots \int_{\Omega_n} \{g\left(z_1, \cdots, z_n\right)\}^k f_{\mathbf{z}}\left(\mathbf{z}\right) d\mathbf{z}$$
$$\simeq \sum_{i_1=1}^{m_1} w_{1 \cdot i_1} \cdots \sum_{i_n=1}^{m_n} w_{1 \cdot i_n} \left\{g\left(l_{1 \cdot i_1}, \cdots, l_{n \cdot i_n}\right)\right\}^k \tag{13}$$

where $f_z(\mathbf{z})$ is the joint p.d.f. of $\mathbf{z}$ and $l_{i \cdot j}, w_{i \cdot j}$ are the j-th node and weight of the i-th variable. Ω_i, m_i are the domain of integration and the number of nodes for i-th variable, respectively. The total number of $g(\mathbf{z})$ evaluations is $m_1 \times m_2 \cdots \times m_n$.

The central moments can be calculated from the raw moments obtained by (13) or directly calculated as in (13) with $g(\mathbf{z})$ replaced by $g(\mathbf{z}) - \mu_g$. Expressions for the mean, standard deviation are as follows:

(mean)

$$\mu_g = \sum_{i_1=1}^{m_1} w_{1 \cdot i_1} \cdots \sum_{i_n=1}^{m_n} w_{n \cdot i_n} g\left(l_{1 \cdot i_1}, \cdots, l_{n \cdot i_n}\right),$$

(STD)

$$\sigma_g = \left[\sum_{i_1=1}^{m_1} w_{1 \cdot i_1} \cdots \sum_{i_n=1}^{m_2} w_{n \cdot i_n} \left(g\left(l_{1 \cdot i_1}, \cdots, l_{n \cdot i_n}\right) - \mu_g\right)^2\right]^{1/2}. \tag{14}$$

With the univariate dimension reduction (UDR) method (Rahman and Xu 2004), the multivariate function $g(\mathbf{z})$ is approximated by a sum of univariate functions which depend on only one variable with the other variables fixed

to their mean values. Let the univariate functions denoted by g_i, then $g(\mathbf{z})$ is approximated as follows:

$$
\begin{aligned}
g(\mathbf{z}) \simeq \hat{g}(\mathbf{z}) &= \sum_{i=1}^{n} g(\mu_1, \cdots, z_i, \cdots, \mu_n) \\
&\quad - (n-1) g(\mu_1, \cdots, \mu_n) \\
&= \sum_{i=1}^{n} g\_i(z_i) - (n-1) g(\mu_{\mathbf{z}}).
\end{aligned} \tag{15}
$$

Here independence of z_i is assumed and it is known that the error of this approximation is mainly contributed from the interaction effects among variables (Xu and Rahman 2004). Since z_i are mutually independent, $g\_i(z_i)$ are also independent with each other and the statistical moments of $\hat{g}(\mathbf{z})$ can be approximated conveniently from moments of $g\_i(z_i)$, as follows (Zhao and Ono 2001):

$$
\text{(Mean)} \quad \mu_{\hat{g}} = \sum_{i=1}^{n} \mu_{g\_i} - (n-1) g(\mu_{\mathbf{z}}),
$$

$$
\text{(Variance)} \quad \sigma_{\hat{g}}^2 = \sum_{i=1}^{n} \sigma_{g\_i}^2. \tag{16}
$$

The moments of univariate functions are calculated using one dimensional Gauss-type quadrature formula. The number of $g(\mathbf{z})$ evaluations for this calculation is $m_1 + \cdots + m_n + 1$ where m_i is the number of nodes used for the calculation of moments of g_i. The UDR method offers a more efficient approach than the TPQ method, however, the method might not be accurate when there exists strong interactions between random variables (Lee and Chen 2008; Lee et al. 2009).

4 Shape derivatives of statistical moments

4.1 Decomposition of the shape derivatives of statistic moments

To minimize the objective functional formulated in (6), we need to quantify the change of the objective functional $J^*(\Omega, u, \mathbf{z})$ with respect to a small variation of the shape Ω (design), which can provide us with necessary information for updating the current design. This process is called shape sensitivity analysis and the result is called shape derivative (Sokolowski and Zolesio 1992). In this section, a semi-analytical shape sensitivity analysis approach is presented for the proposed RSTO formulation. The mean and standard deviation of the response are first numerically discretized using the multivariate Gauss-type quadrature discussed in Section 3.3. From an optimization point of view, the multivariate Gauss-type quadrature essentially transforms the

RSTO problem into a weighted summation of a series of deterministic topology optimization sub problems at the quadrature nodes. The shape sensitivity of each sub problem is then derived using the adjoint variable method and calculus of variation.

Equation (6) can be approximated by using either the TPQ formula in (14) or the UDR formula in (15) and (16). The UDR formula is used here as an example to illustrate how to derive the shape gradient of the statistical moments. For shape sensitivity analysis with TPQ formula, please see our paper (Chen et al. 2009). With the UDR method, the mean and standard deviation of a response are calculated from the mean and standard deviation of univariate sub-functions which can be evaluated by the one dimensional Gauss-type quadrature formula as discussed in Section 3.3. From an optimization point of view, the Gauss-type quadrature formula essentially transforms the RSTO problem into a weighted summation of a series of deterministic topology optimization sub problems. The shape sensitivity of each sub problem is then derived using the adjoint variable method and calculus of variation.

Following this approach, (6) can be approximated as follows by using the UDR formula in (15) and (16).

$$
\begin{aligned}
\mu_J &= \sum_{i=1}^{n} \mu_{J\_i} - (n-1) J(\Omega, \mathbf{u}, \mu_{\mathbf{z}}) \\
\sigma_J^2 &= \sum_{i=1}^{n} \sigma_{J\_i}^2
\end{aligned} \tag{17}
$$

where J_i is a univariate subfunction depending only on one random variable z_i with the other random variables fixed to their mean values; n is the number of random variables. We address the general problem using the variational method and the techniques proposed in Allaire et al. (2004), Pironneau (1984). With the assumption that the random variables are independent of the design variables Ω, the shape derivative of the mean of the performance function $J(\Omega, \mathbf{u}, \mathbf{z})$ is expressed as follows:

$$
D_\Omega[\mu_J] = \sum_{i=1}^{n} D_\Omega\left[\mu_{J\_i}\right] - (n-1) D_\Omega\left[J(\Omega, \mathbf{u}, \mu_{\mathbf{z}})\right] \tag{18}
$$

Similarly, the shape derivative of the standard deviation can be expressed as:

$$
D_\Omega[\sigma_J] = \frac{1}{\sqrt{\sum_{i=1}^{n} \sigma_{J\_i}^2}} \sum_{i=1}^{n} D_\Omega\left[\sigma_{J\_i}^2\right] \tag{19}
$$

The final shape derivative of the objective functional $J^*(\Omega, \mathbf{u}, \mathbf{z})$ is

$$
\begin{aligned}
D_\Omega \left[J^* (\Omega, \mathbf{u}, \mathbf{z}) \right] &= D_\Omega \left[\mu \left(J (\Omega, \mathbf{u}, \mathbf{z}) \right) \right] \\
&\quad + k D_\Omega \left[\sigma \left(J (\Omega, \mathbf{u}, \mathbf{z}) \right) \right] \\
&= \sum_{i=1}^{n} D_\Omega [\mu_{J_{-i}}] \\
&\quad - (n-1) D_\Omega \left[J (\Omega, \mathbf{u}, \mu_\mathbf{z}) \right] \\
&\quad + \frac{k}{\sqrt{\sum_{i=1}^{n} \sigma_{J_{-i}}^2}} \sum_{i=1}^{n} D_\Omega \left[\sigma_{J_{-i}}^2 \right]
\end{aligned}
\tag{20}
$$

With one dimensional Gauss-type quadratue formula, the shape sensitivity $D_\Omega \left[\mu_{J_{-i}} \right]$ and $D_\Omega \left[\sigma_{J_{-i}} \right]$ in (19) and (20) can be calculated from simple mathematical manipulations on the shape sensitivities of a series of deterministic scenarios denoted as $D_\Omega \left[J \left(\Omega, \mathbf{u}, z_{ij} \right) \right]$ $j = 1, \cdots, m_i$ where z_{ij} and m_i mean the j-th quadrature node of z_i and the number of the nodes, respectively. $D_\Omega \left[J \left(\Omega, \mathbf{u}, z_{ij} \right) \right]$ reveals the underlying relations between the design variable shape Ω and the objective functional $J(\Omega, \mathbf{u}, z_{ij})$ under a specified scenario with the random variable z_i.

4.2 Variational method for shape sensitivity analysis of sub problems

In order to calculate (20), we need to calculate the shape sensitivity $J_\Omega(\Omega, \mathbf{u}, z_{ij})$ for each scenario with the random variable z_i. Since in each scenario z_{ij} is constant, we briefly write $J(\Omega, \mathbf{u}, z_{ij})$ as $J(\Omega, \mathbf{u})$ in the following derivation process. Each sub problem can be considered as a deterministic optimization problem, where an objective functional is maximized or minimized with respect to a class of admissible boundaries of the design (Pironneau 1984). The performance functional $J(\Omega, \mathbf{u})$ can be formulated either directly as a domain/boundary integrals as (21) or indirectly formulated as a function of the integrals.

$$
\begin{aligned}
J(\Omega, \mathbf{u}) &= \int_\Omega f(\mathbf{u}(\Omega)) d\Omega \\
J(\Omega, \mathbf{u}) &= \int_{\partial\Omega} f(\mathbf{u}(\Omega)) ds
\end{aligned}
\tag{21}
$$

For example, in the structure optimization problem, the objective functional of mean compliance can be expressed as

$$
J(\Omega, \mathbf{u}) = \int_\Omega \varepsilon(\mathbf{u}) : \mathbf{D} : \varepsilon(\mathbf{u}) d\Omega,
\tag{22}
$$

where $\varepsilon(\mathbf{u}) = \frac{1}{2} \left(\nabla\mathbf{u} + \nabla\mathbf{u}^T \right)$ is the strain field. In linear compliant mechanism optimization problem as demonstrated in one of our examples, geometric advantage (GA)

is a commonly used performance index, which can be formulated as follows (Wang et al. 2005):

$$
\begin{aligned}
GA(\Omega, \mathbf{u}) &= -\frac{\Delta_{out}(\Omega, \mathbf{u})}{\Delta_{in}(\Omega, \mathbf{u})} \\
&= \frac{F_{in}u_{1o} + f_o u_{2o}}{-F_{in}u_{1i} - f_o u_{2i} - F_{in}k u_{1o}u_{2i} + F_{in}k u_{1i}u_{2o}},
\end{aligned}
\tag{23}
$$

where

$$
\begin{aligned}
u_{1i} &= \int_\Omega \varepsilon(\mathbf{u}_1) : \mathbf{D} : \varepsilon(\mathbf{u}_1) d\Omega, \\
u_{2o} &= \int_\Omega \varepsilon(\mathbf{u}_2) : \mathbf{D} : \varepsilon(\mathbf{u}_2) d\Omega, \\
u_{1o} &= u_{2i} = \int_\Omega \varepsilon(\mathbf{u}_1) : \mathbf{D} : \varepsilon(\mathbf{u}_2) d\Omega.
\end{aligned}
\tag{24}
$$

$\mathbf{u}_1$ denotes the displacement field caused by a unit input force; $\mathbf{u}_2$ is the displacement field caused by a unit output force. For more details, please be referred to literatures (Wang et al. 2005).

Assuming Ω is a region with a continuous and smooth boundary, a smooth vector field V is applied along the boundary for an extremely short dummy time τ, mapping Ω into Ω^τ. The variation of the objective functional $J(\Omega, \mathbf{u})$ can be formally defined as follows (Pironneau 1984):

$$
\delta J \stackrel{\Delta}{=} J \left(\Omega^\tau, \mathbf{u} \left(\Omega^\tau \right) \right) - J(\Omega, \mathbf{u}) = [J_\Omega + J_u \mathbf{u}_\Omega] \delta\Omega,
\tag{25}
$$

where the first term in the brackets is the derivative of $J(\Omega, \mathbf{u})$ with respect to Ω with the state variable $\mathbf{u}$ being constant. In terms of the domain-based objective functional $J(\Omega, \mathbf{u}) = \int_\Omega f(\mathbf{u}(\Omega)) d\Omega$, its variation is written as:

$$
\delta J = \int_{\delta\Omega} f(\mathbf{u}) d\Omega + \int_\Omega \delta f(\mathbf{u}) d\Omega.
\tag{26}
$$

According to Sokolowski and Zolesio (1992), Pironneau (1984), the first term in the above equation can be written as

$$
\int_{\delta\Omega} f(\mathbf{u}) d\Omega \doteq \int_{\partial\Omega} f(\mathbf{u}) \mathbf{V} \cdot \mathbf{n} ds.
\tag{27}
$$

Substituting it into (26), we can get

$$
\delta J = \int_{\partial\Omega} f(\mathbf{u}) \mathbf{V} \cdot \mathbf{n} ds + \int_\Omega \delta f(\mathbf{u}) d\Omega.
\tag{28}
$$

In terms of the boundary-based functional $J(\Omega, \mathbf{u}) = \int_{\partial\Omega} f(\mathbf{u}(\Omega)) ds$, its variation has the following form (Sokolowski and Zolesio 1992):

$$
\delta J = \int_{\partial\Omega} \mathbf{V} \cdot \mathbf{n} \left(\frac{\partial f}{\partial n} + f\kappa \right) ds + \int_{\partial\Omega} f_u \delta\mathbf{u} ds.
\tag{29}
$$

where $\frac{\partial f}{\partial n} = \nabla f \cdot \mathbf{n}$ and $\kappa = divn$ is the curvature of a point on the boundary.

The significant challenge in the above equations is that we can not acquire $\mathbf{u}_\Omega$ (or $\delta\mathbf{u}$) directly, since u is a variational weak solution to the state equations. The adjoint variable method is employed in this work to solve this problem. Let $W(\Omega, \mathbf{u}, \mathbf{v}) = 0$ denote the weak form of the physics governing equation. In this work, we only consider linear elastic problems, where the governing equation can be expressed as follows:

$$W(\Omega, \mathbf{u}, \mathbf{v}) = \frac{1}{2}\int_\Omega \varepsilon(\mathbf{u}) : \mathbf{D} : \varepsilon(\mathbf{v})d\Omega$$
$$- \int_\Omega \mathbf{f} \cdot \mathbf{v}d\Omega - \int_{\Gamma_t} \mathbf{g} \cdot \mathbf{v}ds \equiv 0 \quad (30)$$

The variation of the Lagrange equation of the sub problem can be formulated as follows (Arian and Ta'asan 1995):

$$\delta L = \delta J + \delta W = [J_\Omega + J_\mathbf{u}\mathbf{u}_\Omega + \lambda(W_\Omega + W_\mathbf{u}\mathbf{u}_\Omega)]\delta\Omega$$
$$= (J_\Omega + \lambda W_\Omega)\delta\Omega + (J_\mathbf{u} + \lambda W_\mathbf{u})\mathbf{u}_\Omega\delta\Omega \quad (31)$$

By solving the adjoint equation $J_\mathbf{u} + \lambda W = 0$, we can get a proper Lagrange multiplier λ and further get the shape derivative in (20). For more details of sensitivity analysis for level-set based topology optimization, please be referred to literatures (Wang et al. 2003, 2005; Allaire et al. 2004; Chen et al. 2005).

5 RSTO algorithm and demonstration examples

5.1 Numerical algorithm

The algorithm for RSTO is represented by a flowchart shown in Fig. 4. After setting the initial design and boundary conditions, the spectral methods introduced in Section 2 are first applied to reduce the dimensionality for representing the uncertainties in loading and material. For the reduced set of random variables, the locations and weights of nodes are determined next based on the Gauss-type quadrature for calculating the mean and standard deviation of the performance function. The shape sensitivity is then calculated at each integration node. Therefore, the computational cost is proportional to the number of nodes. The velocity field is set using the steepest descent method and the geometry is updated via Hamilton–Jacobi equation. These final two steps are the same as the techniques used for deterministic level set based topology optimization. This loop will iterate until the convergence criterion is satisfied.
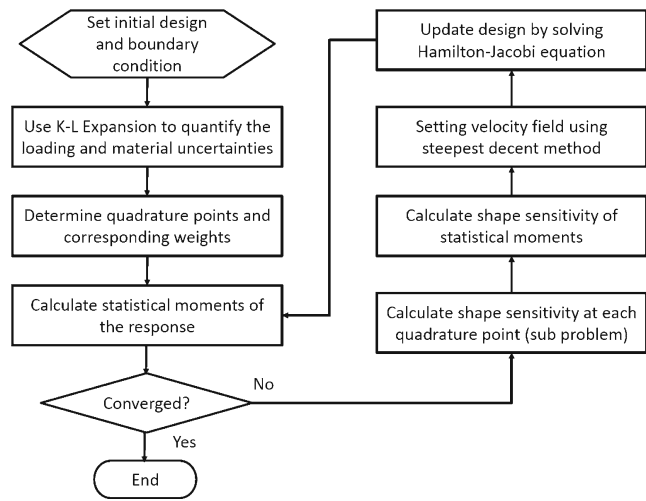

Fig. 4 Flow chart of the RSTO algorithm

5.2 Demonstration examples

The proposed robust design procedure is first applied to an example with two non-normal random variables to verify the effectiveness and feasibility of the moment calculation based on the Gauss-type quadrature formula and the proposed design sensitivity analysis. After that, we apply the proposed method to design a 3D bridge beam with consideration of a random loading field in Example 2 and a random material field in Example 3. In Example 4, a compliant mechanism is designed against the variations associated with a random material field.

Example 1 A 2D bridge beam with a random load at bottom

In this example, a 2D bridge beam structure is optimized with consideration of a random force, of which the magnitude and angle are characterized by two uncorrelated random variables. This example is used to demonstrate the geometric differences between the robust design and its deterministic counterpart, their respective performances under the random force, and the accuracy of statistical moments computed using the proposed uncertainty propagation techniques.

The robust design objective is to minimize the weighted summation of the mean and standard deviation of the total strain energy of the structure as introduced in (6), where the weight k for minimizing the standard deviation is set to be 1 in all examples in this paper, assuming optimizing an mean performance is equally important as minimizing its standard deviation. The boundary condition of the bridge beam is shown in Fig. 6. The design domain is defined within a 2-by-1 square with the lower left corner fixed and the lower right corner simply supported. A random external force is

applied in the middle of the bottom. The angle θ takes a uniform distribution (32) with the interval from $-\frac{3\pi}{4}$ to $-\frac{\pi}{4}$,

$$p(\theta) = \begin{cases} \dfrac{2}{\pi} & \theta \in \left[-\dfrac{3\pi}{4}, -\dfrac{\pi}{4} \right] \\ 0 & else \end{cases} . \quad (32)$$

The force magnitude h takes a Gumbel distribution (33) which is an extreme value distribution used to consider the rare events of very large force magnitudes,

$$p(h) = \frac{1}{\sigma} \exp\left[-\frac{h-\mu}{\sigma} - \exp\left(-\frac{h-\mu}{\sigma} \right) \right], \quad (33)$$

where the mean (location parameter) μ is equal to 1 and the standard deviation (distribution scale) σ is equal to 0.3. The plot of the joint PDF (probability density function) is shown in Fig. 5a.

The level set function is evolved on a 401-by-201 fixed Eulerian grid. The design domain is discretized using 100-by-50 finite elements for elastic analysis. The elastic material is assumed with a dummy Young's modulus of $E = 1$ and the Poisson ratio of 0.3. The void area is assumed with a dummy Young's modulus of 0.001 and the same Poisson ratio of 0.3. A volume constraint is applied with a fixed Largrangian multiplier of 1,000 (Allaire et al. 2004). The settings in the deterministic optimization are the same as the robust optimization example, except that the load is a deterministic unit force ($f = -1$) in the vertical direction.

As shown in Fig. 5b, a 25-point tensor product Gauss-type quadrature is used to identify the locations and corresponding weights of the quadrature nodes for the two random variables and then calculate the mean and standard deviation of the compliance at each design solution.

As shown in Fig. 6, the geometric difference between the robust and deterministic designs is obvious. The robust design possesses an asymmetrical configuration while its deterministic counterpart is characterized by a strictly symmetric pattern. These solutions match well with the
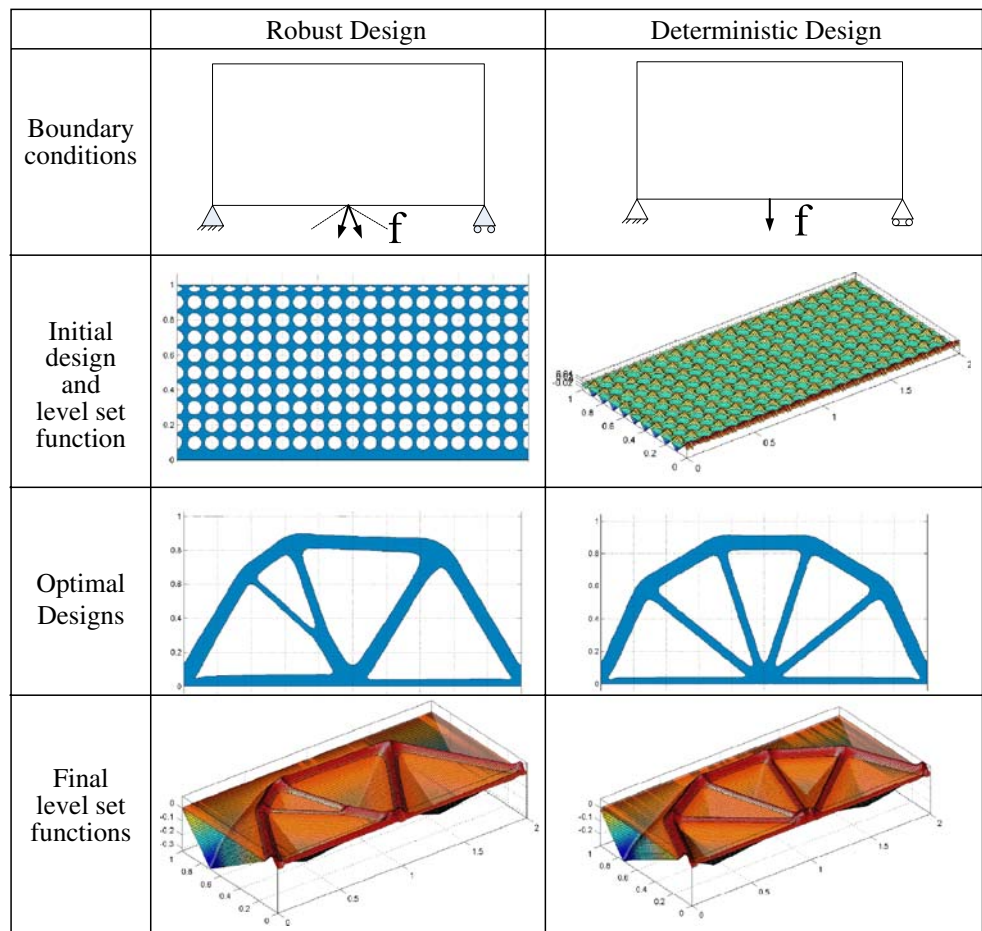
problem formulations. In particular, the deterministic design is a symmetric design because the vertical load is applied in the middle of the bottom structure and the vertical displacements are constrained symmetrically at both the lower left and the lower right corners. In robust design, due to its randomness, the applied force may pose a horizontal component on the structure, resulting an asymmetrical boundary condition. Considering that only the lower left corner is fixed while the lower right corner is movable in the horizontal direction, the left half structure undergoes an additional deformation caused by the horizontal force, leading to an asymmetrical design. It can be noted that the robust design possesses a thicker bottom chord at the lower left side than the one at the right side, which provides additional stiffness to withstand the deformation caused by the horizontal force component.

For the purpose of verification, the mean performance and robustness (standard deviation) of the robust and deterministic designs are compared in Table 1, subject to the same random load. To verify the accuracy of the 25-point tensor product Gauss-type quadrature formulae, results from 10,000 Monte Carlo simulations are used as reference. By using the linear superposition theory, the computational cost is significantly reduced for running the Monte Carlo simulations. For the given random load, both the mean (1,410.70) and standard deviation (994.86) of the robust topology design are much smaller (better) than those of the deterministic design (1,422.25 and 1,030.93 respectively). Therefore even though the deterministic topology optimization solution optimizes its performance (compliance $C = 1,371.86$) for a deterministic load condition, the robust topology design possesses a superior performance and better robustness with respect to a range of load conditions with varying magnitudes and directions. It is noted from Table 1 that the statistical performance obtained from the 25-point tensor product Gauss-type quadrature formulae are very close to those of the Monte Carlo method, with much improved efficiency. It is also noted that the robust and deterministic designs possess similar volume ratios (0.246 and 0.247).

Fig. 5 Visualization of the joint PDF of the force (**a**) and the locations of TPQ nodes with corresponding weights (**b**)
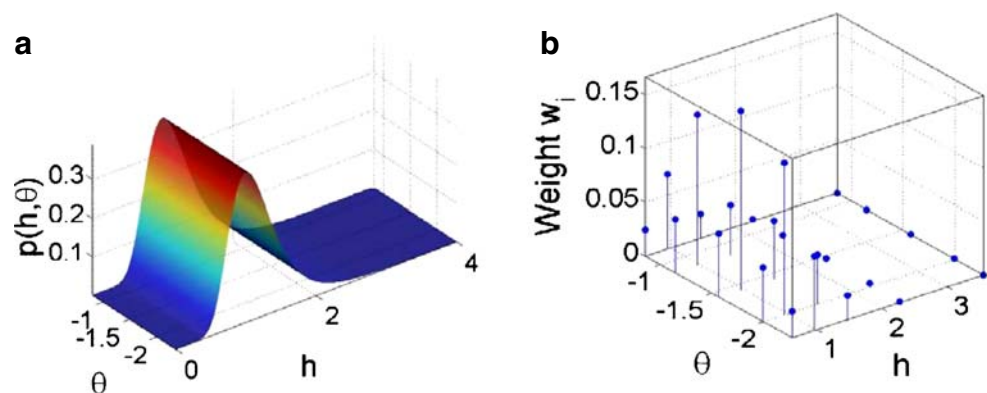
Fig. 6 Robust (*left column*) vs. deterministic (*right column*) topology optimization of a beam structure

	Robust Design	Deterministic Design
Boundary conditions		
Initial design and level set function		
Optimal Designs		
Final level set functions		

Example 2 A 3D bridge beam with a random loading field at the top

In this example, we optimize a 3D bridge beam considering a random loading field on the top. Here the load is considered as a random field because the correlations of the random load exist at different locations of the bridge beam top surface. The robust design objective is to optimize the weighted summation of the mean and standard deviation of the total strain energy. To verify the method, solutions from the following there scenarios are compared: (1) RSTO solution for the given random loading field, (2) an optimal design under a deterministic, distributed constant load, and

(3) an optimal design under distributed random variable load where the load magnitude is treated as a random variable everywhere.

The boundary conditions and initial designs are shown in Fig. 7a, b. The dimensions of the design domain are 2-by-0.5-by-1 (X-by-Y-by-Z). The lower left corner of the design domain is fixed and the lower right corner is simply supported. A distributed load is applied at the top. For scenario (1), the load magnitude at each point is assumed to take a normal distribution with mean equal to 1 and standard deviation equal to 0.2; the correlation length of the random field is set to be 0.15. For scenario (2), the magnitude of the deterministic distributed constant load is set as 1. For scenario

Table 1 Comparison between robust and deterministic designs

		Robust	Deterministic
$\mu(C)$	25-point tensor-product quadrature	1,410.70	1,422.25
	Monte Caro (10,000 points)	1,400.10	1,424.99
$\sigma(C)$	25-point tensor-product quadrature	994.86	1,030.93
	Monte Caro (10,000 points)	959.86	1,042.93
Volume ratio		0.246	0.247

C mean compliance of the structure

Fig. 7 Scenario (1)—RSTO of a 3D bridge beam subject to random loading field. **a** 2D sketch of the boundary conditions, **b** initial design and loading condition, **c** final design, **d** isometric view from another viewpoint
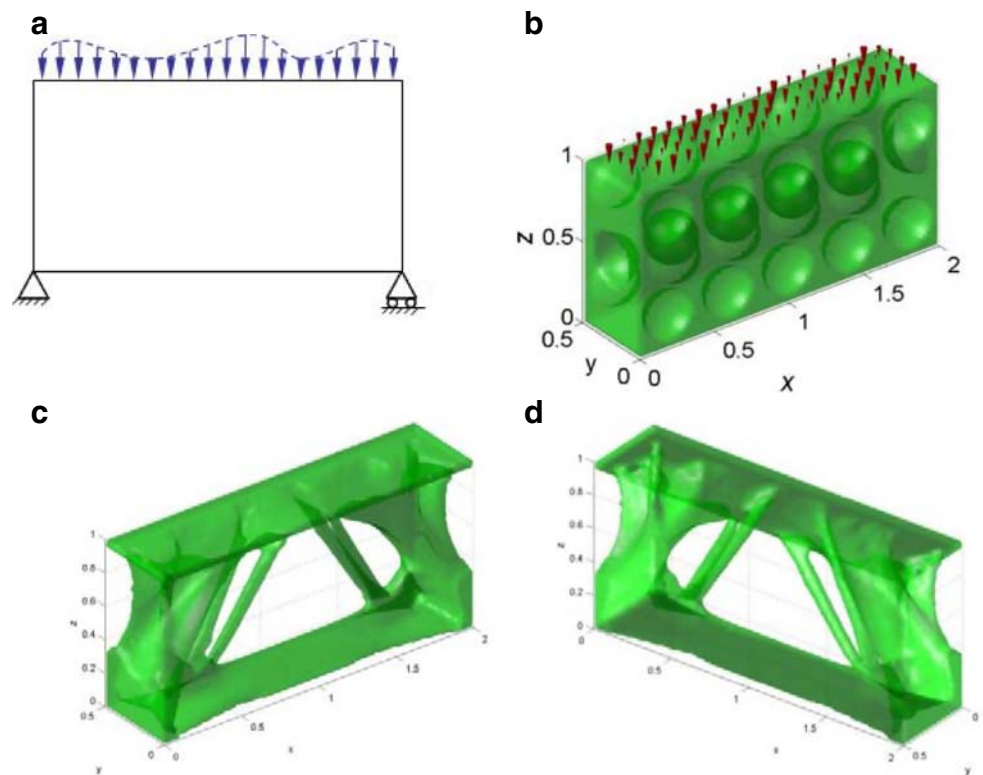
(3), the magnitude of the distributed random variable load follows the distribution $N(1, 0.2)$everywhere.

In the optimization process, the level set function is evolved on a 161-by-41-by-81 fixed Eulerian grid, where the design domain is discretized using about 14,000 finite elements for elastic analysis. For scenario (1), nine eigenvectors are identified in the reduced K–L expansion and used in uncertainty quantification, while three quadrature nodes are used in the direction of each eigenvector. UDR is employed to calculate the stochastic moments, which reduces the finite element evaluation numbers from 27 (using the tensor product quadrature) to 19 in each optimization iteration.

The final design of RSTO under a random loading field (Scenario (1)) is shown in Fig. 7c, d. The deterministic result (Scenario (2)) is shown in Fig. 8a, b; the robust design with a random variable load (Scenario (3)) is shown in Fig. 8c, d. Compared with the deterministic design (Scenario (2)), the robust designs with the random field (Scenario (1)) or random variable models (Scenario (3)) possess more bars and a thicker beam at bottom, which provide additional strengths to the bridge under loading variations. Comparing the two robust designs (Scenarios (1) and (3)), we find that the configurations of the two designs are similar, indicating that the spatial variability of load does not have a significant impact on the result for this case study. In essence, the conventional single-random-variable model can be considered as a special case of the random

field model. A comparison of the mean and standard deviation of the designs are listed in Table 2, showing that the design with the random field model (Scenario (1)) achieves slightly better performance in its mean and standard deviation compared to the random variable model (Scenario (3)).

Example 3 A 3D bridge beam with a random material field

In this problem, a 3D bridge beam is optimized subject to a spatially-varying material property field across the design domain. The objective function is still to optimize the weighted summation of the mean and standard deviation of the total strain energy of the structure. The boundary condition of the problem is similar to that of example 1 and the dimensions of the design domain are the same as the setting of example 2. The material property field (Young's Modulus) is assumed to take a normal distribution with mean equal to 1 and standard deviation 0.2. A realization of the random field is shown in Fig. 9b. An exponential function is employed to describe the correlation between any two spatial points in the random field as follows:

$$C = \exp\left(-\frac{\|X_1 - X_2\|}{d}\right). \tag{34}$$

Here $\|X_1 - X_2\|$ is the Euclidean distance between the two points and d is the correlation length which is set to be 0.5 in this example. In the optimization process, the level set

Fig. 8 Topology optimization of a 3D bridge beam considering Scenario (2)—distributed constant load and Scenario (3) a distributed random variable load. **a** Scenario (2)—deterministic design under distributed constant load, **b** isometric view of the deterministic design from another viewpoint, **c** Scenario (3)—robust design considering a distributed random variable load, **d** isometric view of robust design from another viewpoint
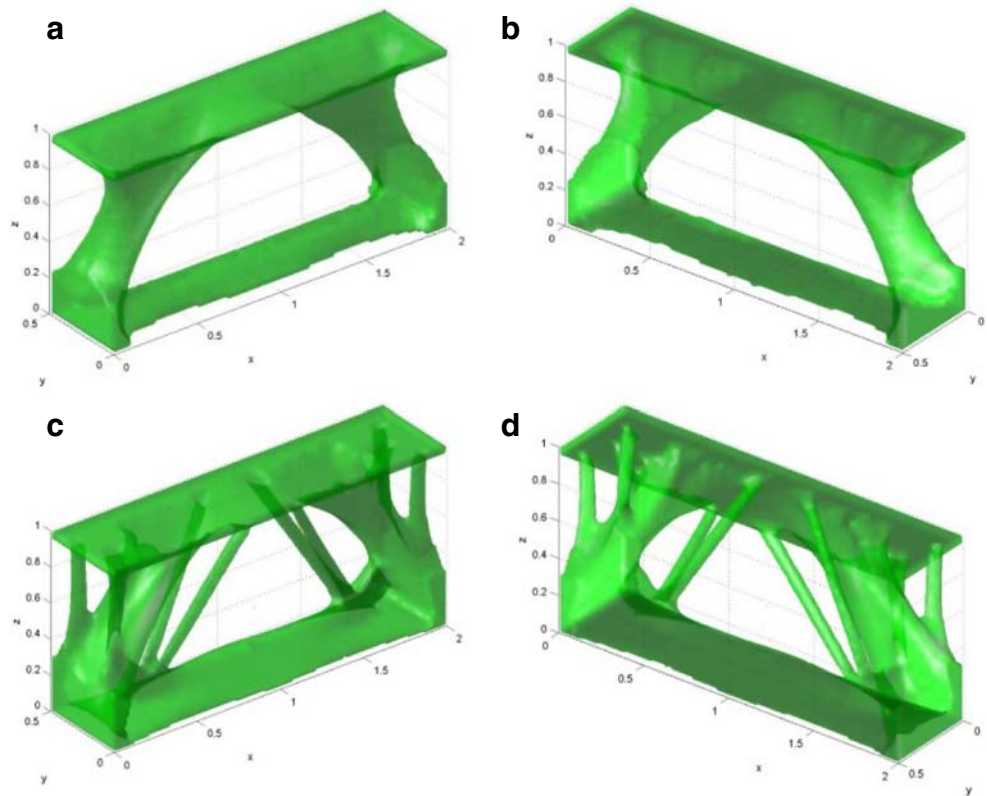
function is evolved on a 101-by-21-by-51 fixed Eulerian grid, and the design domain is discretized using about 4,000 finite elements for elastic analysis. Due to the strong correlation, three eigenvectors are used in uncertainty quantification and the random material field can be quantified as follows:

$$g(x, \omega) = \bar{g}(x) + \sum_{i=1}^{3} \sqrt{\lambda_i} g_i(x) \xi_i(\omega). \tag{35}$$

Three quadrature nodes are used in each eigenvector direction for demonstration. The final design of RSTO is shown in Fig. 9c, d. The corresponding DTO results are shown in Fig. 9e, f, where the Young's Modulus is a constant 1.

Since the material random field is geometry dependent and the optimal geometry from robust optimization is

Table 2 Comparison of designs under a random loading field, a distributed random load and a distributed constant load

|	Random field	Single random variable	Deterministic
$\mu(C)$	8.7420	9.1757	8.0384
$\sigma(C)$	2.0463	3.5533	
Volume ratio	0.27	0.26	0.25

C mean compliance of the structure

different from that of deterministic design, it is not appropriate to directly compare the performances between the two designs. Even so, we can still evaluate the robustness of a design by associating its geometric model with different material property fields and calculating its (mean) performances under different scenarios. If the (mean) performances of the design do not change much under different material property fields, it means the geometric design possesses good robustness. In this example, we apply a constant material field and a random material field to the robust and deterministic designs respectively. The performances of robust and deterministic designs under two material property fields are listed in Table 3. According to Table 3, the mean compliance of the robust design does not change much (23.05 to 23.25) under different material fields, while the mean compliance of the deterministic design degrades (22.73 to 23.48) when changing from a constant material field to a random field. This indicates that the robust design is less sensitive to the variations of material properties although its performance is not so good as the deterministic design under a constant material field, which coincides well with our anticipation. From a geometric point of view, the robust design possesses obviously thicker bars while the number of bars is less than that of its deterministic counterpart, making the appearance more robust. The increased thickness of the bars makes the robust design less sensitive to the variations in the material field.

Fig. 9 Robust (**a**–**d**) vs. deterministic (**e**, **f**) optimization of a 3D bridge beam under a random material field. **a** Initial design, **b** a realization of the random material field, **c** robust design, **d** isometric view of the robust design from another viewpoint, **e** deterministic design, **f** isometric view of the deterministic design from another viewpoint
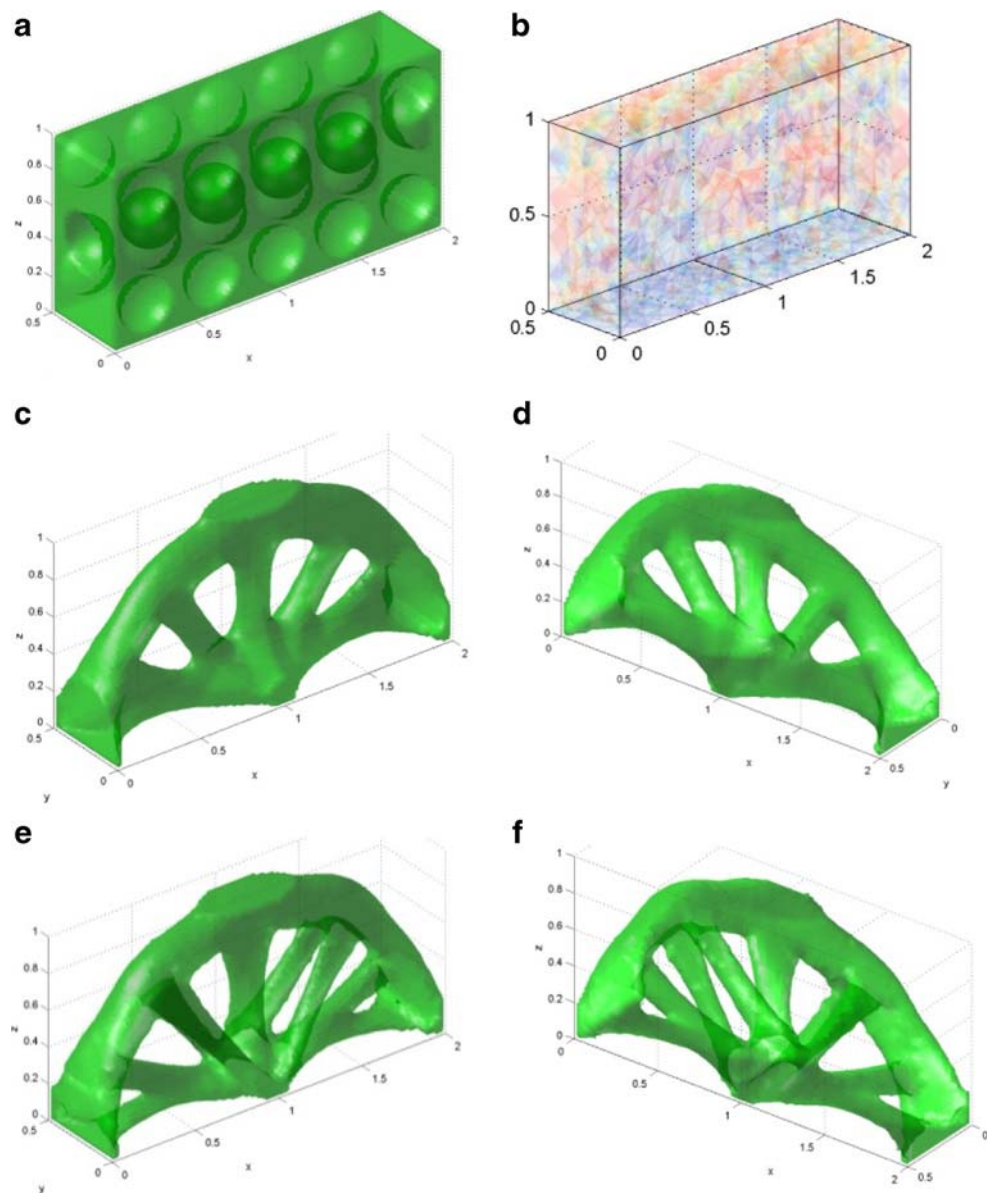
Example 4 Designing A 3D micro-gripper under a random material field

A 3D micro-gripper, subject to a spatially-varying material property field across the design domain, is used as an example to demonstrate the proposed method to robust compliant mechanism design. The boundary conditions of the deterministic and robust designs are the same, which are shown in Fig. 10a: the four corners of the left side are fixed; a horizontal force is applied at the center of the left side; two vertical output displacements are expected at ports 1 and 2. The design objective in a deterministic compliant mechanism optimization problem is to minimize the geometric advantage (GA), which is defined as the ratio of the output displacement over the input displacement. More details about setting a compliant mechanism optimization

Table 3 Compliances of robust and deterministic designs under different material property fields

C mean compliance of the structure

	Parameters of material fields	Robust design	Deterministic design
Deterministic material field	$E=1$	C = 23.05	C = 22.73
Random material field	$\mu_E = 1, \sigma_E = 0.2, d = 0.5$	$\sigma(C) = 23.25$	$\sigma(C) = 23.48$
Volume ratio		0.24	0.23

Fig. 10 Robust (**c**, **d**) vs. deterministic (**e**, **f**) optimization of a 3D micro-gripper under a random material field. **a** Boundary condition, **b** initial design, **c** robust design, **d** isometric view of the robust design from another viewpoint, **e** deterministic design, **f** isometric view of the deterministic design from another viewpoint
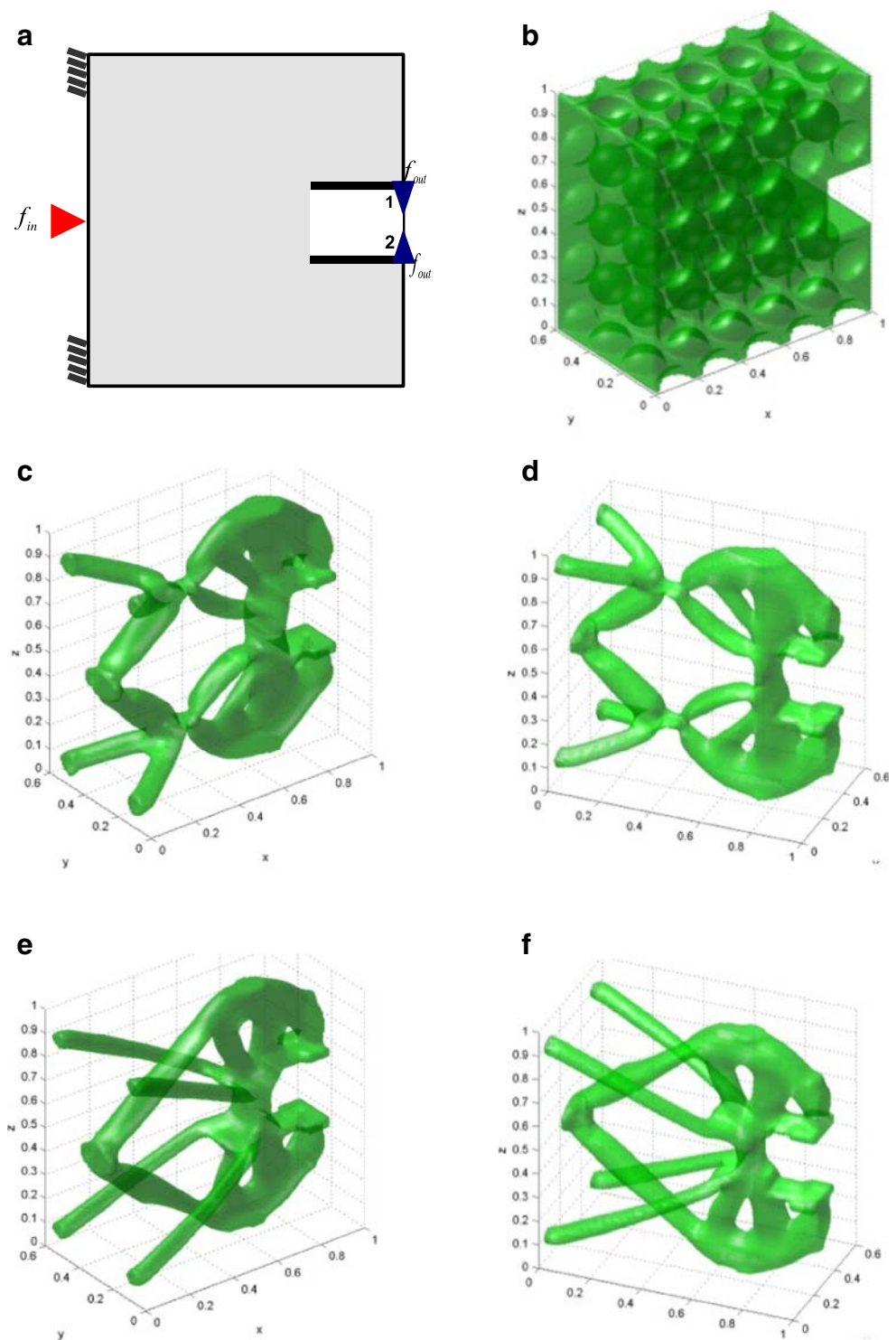
problem can be found in Wang et al. (2005), Wang and Chen (2009), Chen et al. (2005), Chen and Wang (2006). The corresponding objective function of the RSTO problem is to optimize the weighted summation of the mean and standard deviation of the GA. The dimensions of the design domain are 1-by-0.6-by-1. The material property field (Young's Modulus) is assumed to take a normal distribution with mean equal to 1 and standard deviation 0.3. The correlation function and the correlation length d of the random field are the same as those of example 3. For simplicity, it is assumed that the random field follows the symmetry, hence only the upper part of the design is analyzed in

Table 4 Comparison of robust and deterministic CM designs under different material property fields

	Parameters of material fields	Robust design	Deterministic design
Material field 1	$E = 1$	GA = −0.065	GA = −0.070
Material field 2	$\mu_E = 1, \sigma_E = 0.3, d = 0.5$	μ(GA) = −0.059	μ(GA) = −0.055
Volume ratio		0.098	0.090

the optimization process. The level set function is evolved on a 101-by-61-by-51 fixed Eulerian grid, and the design domain is discretized using about 5,000 finite elements for elastic analysis. Similar to example 3, three eigenvectors are used in uncertainty quantification based on reduced K–L expansion, and three quadrature nodes are used in each eigenvector direction based on the UDR method. The final design of RSTO is shown in Fig. 10c, d. The corresponding deterministic optimization result is shown in Fig. 10e, f, where the Young's Modulus is set as a constant 1. Similar to example 3, for the purpose of verification, we apply two different material fields to the robust and deterministic designs respectively to evaluate their robustness under different material fields. The performances of robust and deterministic designs are listed in Table 4. According to Table 4, the geometric advantage of the robust design is more stable (−0.065 to −0.059) under different material fields, while the geometric advantage of the deterministic design degenerates (−0.070 to −0.055) when the material property field varies. This comparison shows that the robust compliant mechanism design possesses superior robustness than its deterministic counterpart under different material property fields. Comparing the geometries of the robust and deterministic designs, we find the robust design consists of shorter but obviously thicker bars than its deterministic counterpart. Since the local stress constraint is not taken into account in current research, the obtained robust design is more of a lumped compliant mechanism composed of rigid parts connected by de facto hinges. The short and thick bars favor the robust design objective function, making the robust design less sensitive to material property variations. The deterministic design possesses long and slim bars the strength of which is more sensitive to material property variations. But there are less de facto hinges which makes the stress level lower than its robust counterpart.

method provides a mathematically rigorous and computationally viable approach to RSTO problems. It also offers a unified framework for both robust shape and topology optimization, that is applicable to various applications. To reduce the dimensionality in characterizing random field uncertainty, the Karhunen–Loeve expansion is employed with a reduced set of random variables. Based on the total number of random variables and the existence of variant interactions, either the TPQ rule or the UDR quadrature rule is then employed for calculating statistical moments of the design response. The Gauss-type quadrature essentially transforms the RSTO problem into a weighted summation of a series of deterministic topology optimization sub problems at the quadrature nodes. This enables a semi-analytical approach that introduces the shape sensitivity of the statistical moments using the adjoint variable method and calculus of variation. The shape derivative is seamlessly integrated with a conventional level-set-based topology optimization framework via the steepest descent method. The proposed RSTO method is illustrated with bench mark examples subject to lumped random loads and a random loading/material field. The benchmark examples show that the results from RSTO may be quite different from that of the deterministic topology optimization and the RSTO designs are more robust than deterministic designs under uncertainty. Although the current contents of this paper are focused on Gauss-type loading and material uncertainties, the proposed method is generic and can be easily extended to robust topology optimization subject to other types of uncertainties, such as Gauss/Non-Gauss type geometric uncertainties. Throughout our research, we also had the observation that uncertainty is not the only factor that has impact on the topology of the final design; the interaction between the boundary condition and the uncertainties determines the topology of the final design to a large extent (keeping other conditions fixed). These issues still require further investigations in our future research.

6 Conclusions and future work

The paper presents a unique approach to implement robust design to level set based shape and topology optimization with the consideration of random field uncertainty. The

References

Allaire G, Jouve F, Toader A-M (2002) A level-set method for shape optimization. C R Acad Sci Paris Serie I 334:1–6

Allaire G, Jouve F, Toader AM (2004) Structural optimization using sensitivity analysis and a level-set method. J Comput Phys 194:363–393

Allen M, Maute K (2005) Reliability-based shape optimization of structures undergoing fluid–structure interaction phenomena. Comput Methods Appl Mech Eng 194(30–33):3472–3495

Arian E, Ta'asan S (1995) Shape optimization in one-shot. In: Boggaard J et al (eds) Optimal design and control. Birkhauser, Boston, pp 273–294

Bendsøe MP, Kikuchi N (1988) Generating optimal topologies in structural design using a homogenization method. Comput Methods Appl Mech Eng 71:197–224

Bendsøe MP, Ben-Tal A, Zowe J (1994) Optimization methods for truss geometry and topology design. Struct Multidiscipl Optim 7:141–159

Beyer H-G, Sendhoff B (2007) Robust optimization—a comprehensive survey. Comput Methods Appl Mech Eng 196(33–34):3190–3218

Birge J, Louveaux F (1997) Introduction to stochastic programming. Springer, New York

Chen SK, Wang MY (2006) Conceptual design of compliant mechanisms using level set method. Frontiers of Mechanical Engineering in China 1(2):131–145

Chen SK, Wang MY (2007) Designing distributed compliant mechanisms with characteristic stiffness. In: of the ASME 2007 international design engineering technical conferences and computers and information in engineering conference IDETC/CIE 2007. Las Vegas, Nevada, USA

Chen W, Allen JK, Tsui KL, Mistree F (1996) A procedure for robust design: minimizing variations caused by noise factors and control factors. ASME J Mech Des 18(4):478–485

Chen SK, Wang MY, Liu AQ (2008) Shape feature control in structural topology optimization. Computer-Aided Des 40(9):951–962

Chen SK, Wang MY, Wang SY (2005) Optimal synthesis of compliant mechanisms using a connectivity preserving level set method. In: of ASME 2005 international design engineering technical conferences and computers and information in engineering conference, 31st design automation conference. Long Beach, CA

Chen S, Lee S, Chen W (2009) Level set based robust shape and topology optimization under random field uncertainties. In: ASME 2009 international design engineering technical conferences and computers and information in engineering conference. San Diego, California, USA

Christiansen S, Patriksson M, Wynter L (2001) Stochastic bilevel programming in structural optimization. Struct Multidiscipl Optim 21(5):361–371

Conti S, Held H, Pach M, Rumpf M, Schultz R (2008) Shape optimization under uncertainty—a stochastic programming perspective. SIAM J Optim 19(4):1610–1632

Du X, Chen W (2000) Towards a better understanding of modeling feasibility robustness in engineering design. ASME J Mech Des 122:385–394

Du X, Chen W (2001) A most probable point based method for uncertainty analysis. J Des Manuf Autom 4:47–66

Engels H (1980) Numerical quadrature and cubature. Academic, London

Ghanem RG, Doostan A (2006) On the construction and analysis of stochastic models: characterization and propagation of the errors associated with limited data. J Comput Phys 217:63–81

Ghanem RG, Spanos PD (1991) Stochastic finite elements: a spectral approach. Springer, New York

Haldar A, Mahadevan S (2000) Reliability assessment using stochastic finite element analysis. Wiley, New York

Jin R, Du X, Chen W (2003) The use of metamodeling techniques for optimization under uncertainty. J Struct Multidiscipl Optim 25(2):99–116

Jung H-S, Cho S (2004) Reliability-based topology optimization of geometrically nonlinear structures with loading and material uncertainties. Finite Elem Anal Des 41(3):311–331

Kalsi M, Hacker K, Lewis K (2001) A comprehensive robust design approach for decision trade-offs in complex systems design. J Mech Des 123(1):1–10

Kharmanda G, Olhoff N (2002) Reliability-based topology optimization as a new strategy to generate different structural topologies. In: 15th Nordic seminar on computational mechanics. Aalborg, Denmark

Kharmanda G, Olhoff N, Mohamed A, Lemaire M (2004) Reliability-based topology optimization. Struct Multidiscipl Optim 26(5):295–307

Kogiso N, Ahn W, Nishiwaki S, Izui K, Yoshimura M (2008) Robust topology optimization for compliant mechanisms considering uncertainty of applied loads. J Adv Mech Des Syst Manufac 2(1):96–107

Lee SH, Chen W (2008) A comparative study of uncertainty propagation methods for black-box type functions. Struct Multidiscipl Optim 37(3):239–253

Lee SH, Chen W, Kwak BM (2009) Robust design with arbitrary distributions using Gauss-type quadrature formula. Struct Multidiscipl Optim 39(3):227–243

Maute K, Frangopol DM (2003) Reliability-based design of MEMS mechanisms by topology optimization. Comput Struct 81:813–824

Melchers RE (1999) Structural reliability analysis and prediction. Wiley, Chichester

Mogami K et al (2006) Reliability-based structural optimization of frame structures for multiple failure criteria using topology optimization techniques. Struct Multidiscipl Optim 32(4):299–311

Mozumder C et al (2006) An investigation of reliability-based topology optimization techniques. In: Proceedings of the 11th AIAA/ISSMO multidisciplinary analysis and optimization conference, AIAA-2006-7058. AIAA, Portsmouth

Osher S, Fedkiw R (2003) Level sets methods and dynamic implicit surfaces. Springer, New York

Osher S, Sethian J (1988) Fronts propagating with curvature-dependent speed: algorithms based on Hamilton–Jacobi formulations. J Comput Phys 79:12–49

Osher S, Santosa F (2001) Level set methods for optimization problems involving geometry and constraints. I. Frequencies of a two-density inhomogeneous drum. J Comput Phys 171:272–288

Parkinson A, Sorensen C, Pourhassan N (1993) A general approach for robust optimal design. ASME J Mech Des 115(1):74–80

Phadke MS (1989) Quality engineering using robust design. Prentice Hall, Englewood Cliffs

Pironneau O (1984) Optimal shape design for elliptic systems. Series in computational physics. Springer, New York

Rahman S, Xu H (2004) A univariate dimension-reduction method for multi-dimensional integration in stochastic mechanics. Probab Eng Mech 19:393–408

Reddy J (1986) Applied functional analysis and variational methods in engineering. McGraw-Hill, New York

Rozvany GIN, Zhou M, Birker T (1992) Generalized shape optimization without homogenization. Struct Optim 4:250–254

Seepersad CC, Alien JK, Mcdowell DL, Mistree F (2006) Robust design of cellular materials with topological and dimensional imperfections. ASME J Mech Des 128:1285–1297

Sethian JA (1999) Level set methods and fast marching methods, 2nd edn. Cambridge University Press, Cambridge

Sethian JA, Wiengmann A (2000) Structural boundary design via level set and immersed interface methods. J Comput Phys 163: 489–528

Sigmund O (2001) A 99 line topology optimization code written in MATLAB. Struct Multidiscipl Optim 21(2):120–127

Sokolowski J, Zolesio JP (1992) Introduction to shape optimization: shape sensitivity analysis. Springer, New York

Taguchi G (1993) Taguchi on robust technology development: bringing quality engineering upstream. ASME, New York

Wang MY, Chen SK (2009) Compliant mechanism optimization: analysis and design with intrinsic characteristic stiffness. Mech Des Struct Mach 37(2):183–200

Wang MY, Wang XM (2004a) 'Color' level sets: a multi-phase level set method for structural topology optimization with multiple materials. Comput Methods Appl Mech Eng 193:469–496

Wang MY, Wang XM (2004b) PDE-driven level sets, shape sensitivity, and curvature flow for structural topology optimization. Comput Model Eng Sci 6:373–395

Wang MY, Wang XM, Guo DM (2003) A level set method for structural topology optimization. Comput Methods Appl Mech Eng 192:227–246

Wang MY, Chen SK, Wang XM, Mei YL (2005) Design of multi-material compliant mechanisms using level set methods. ASME J Mech Des 127(5):941–956

Wu CFJ, Hamada M (2000) Experiments: planning, analysis, and parameter design optimization. Wiley, New York

Xu H, Rahman S (2004) A generalized dimension-reduction method for multi-dimensional integration in stochastic mechanics. Int J Numer Methods Eng 61:1992–2019

Ying X, Lee S, Chen W, Liu W (2009) Efficient random field uncertainty propagation in design using multiscale analysis. ASME J Mech Des 131(2):021006.1–021006.10

Zabaras N (2007) Spectral methods for uncertainty quantification. Available from: http://mpdc.mae.cornell.edu/

Zhao Y-G, Ono T (2001) Moment methods for structural reliability. J Struct Saf 23:47–75